Control of secondary electron emission coefficient with micro-structural change of polycrystalline MgO films

Hak Ki Yu[1], Jong-Lam Lee[1], Eung Chul Park[2], Jae Sung Kim[2] and Jae Hwa Ryu[2]

[1]**Dept. of Materials Science and Engineering, Pohang University of Science and Technology (POSTECH), Pohang, Kyungbuk 790-784, Korea**

TEL:82-54-279-2152, e-mail: jllee@postech.ac.kr

[2]**LG Electronics Inc., Kumi, Kyungbuk, 730-030, Korea**

Keywords : MgO, Secondary electron emission, oxygen vacancy

Abstract

Micro crystal structure of polycrystalline MgO film is controlled by adjusting the energy of particles arrived at the substrate during deposition. The change of crystal structure affects on the total area of (200) surface where the oxygen vacancies are formed easily, resulting in the change of secondary electron emission (SEE) coefficient (γ).

1. Introduction

F and F^+ centers related to oxygen vacancies of MgO have been of growing interest owing to their role in increasing SEE,[1-4] due to their position in the forbidden band gap of MgO about 3.0eV above valence band maximum (VBM) for F center and 2.96eV above VBM for F^+ center. However, most of the works to form oxygen vacancies of MgO have focused on the doping [3,4] and the control of oxygen partial pressure during growth,[1,2] little attention has been given to the effect of crystal structure on the oxygen vacancy concentration. Because the oxygen vacancies of MgO are formed easily at the surface of (200) plane that has low surface energy, it is very important to increase the (200) surface at the top of MgO film where the secondary electrons are emitted intensively.

The preferred orientation is determined when the overall film energy composed of surface energy and strain energy is minimized. Thus, it could be changed by adjusting surface energy or strain energy of film. In our experiment, we control the preferred orientation of MgO film by controlling growth condition, via, adjusting strain energy. The deposition rate affects on adatom mobility and binding energy between adatoms; resulting in the change of strain energy.

2. Experimental

An n^{++}-type (100) silicon substrate doped with arsenic (resistivity < 0.004 Ω·cm) was used as a starting substrate. The substrate was cleaned with acetone, ethyl-alcohol, and de-ionized water. The native oxide of a Si wafer was removed by HF treatment. MgO films were deposited by electron beam evaporation using high purity MgO pellets. The MgO pellets were made by pressing 99.995 % purity MgO powder (from Mitsubishi Materials Co.) and performing heat treatment. The deposition rate was controlled by emission current of filament. Chamber pressure was maintained at about ~ 10^{-6} Torr during deposition and substrate temperature was held at 250 °C. Gas breakdown voltages were measured using the DC breakdown voltage measurement system. The γ was calculated using the equation,

$$V_b = \frac{B\,p\,d}{\ln\left(\frac{A\,p\,d}{\ln(1+1/\gamma)}\right)}$$

where A and B are gas constants for the ionization rate of gas species. The coefficients used for the Ne gas discharge were A = 4 cm^{-1} $Torr^{-1}$ and B = 100 V / cm Torr. $P \cdot d$ is the Paschen parameter defined by the product of gas pressure P and inter-distance d between the anode and cathode. At each Paschen parameter, GPIB interconnected voltage controller applied voltage from 150 V to breakdown voltage. KITHELEY 487 picoammeter – voltage source detected the current between cathode and anode. In-lab X-ray diffraction is measured by powder X-ray diffractometry (XRD; 18 kW, Mac Science,

M18XHF22) using monochromated Cu Kα radiation and a scintillation detector. Scanning electron microscopy (SEM) is done using a PHILIPS XL30S with an accelerating voltage of 10 kV and a working distance of 5 mm.

3. Results and discussion

Figure 1(a), 1(b) show XRD profiles for the MgO films deposited at high (20Å/s) and low (3Å/s) rates. The diffraction profiles revealed that (200) diffraction peak was dominant at the initial stage and (111) diffraction intensity increased as the film thickness increased for both deposition rates. For the samples deposited at 20Å/s, this tendency is happened at the earlier stage of growth and more distinct. For the rock-salt crystal structure such as MgO, (200) plane is preferred at the initial stage of growth due to lower surface energy. As the film thickness increased, (200) plane is unstable due to accumulation of high strain energy. To stabilize the overall film energy, the preferred orientation is needed to change from (200) plane to (111) plane that has lower strain energy. The change of growth structure from (200) to (111) is accompanied with rapid RMS increase (*not shown here*). The origin of rapid RMS increase is the formation of tetrahedron enclosed with the family plane of (200). In other words, growth direction is changed from (200) to (111) direction to reduce strain energy and surface termination is maintained with (200) and their family plane that has the lowest surface energy. The tetrahedron is shown in the Fig. 2 clearly. As the deposition rate decreased from 20Å/s to 3Å/s, the size of tetrahedron decreased and the total area of (200) surface increased.

Figure 3 shows the mean Paschen curves of MgO films with deposition rate. The breakdown voltage measurement was carried out at a constant distance of 3 mm gap between the Cu anode and MgO cathode. $P{\cdot}d$ values were controlled by changing the pressure of Ne (10% Xe mixed) gas from 3 Torr to 20 Torr. At a given $P{\cdot}d$ value of 4.2 Torr·cm (dotted line in Fig. 3.) corresponding to general PDP operation condition in PDP discharges, the breakdown voltage of the samples deposited at 20Å/s was 267 V. As the deposition rate decreased from 20Å/s to 3Å/s, the breakdown voltage decreased to 248 V. The change of γ with deposition rate calculated from the Paschen relation. The γ values match with 4.2 Torr cm were calculated to be 0.048 for 3 Å/s, 0.046 for 5 Å/s, 0.034 for 10 Å/s, and 0.032 for 20 Å/s, respectively. The increase of SEE coefficient at the low deposition rate (3 Å/s) is deeply related to the increase of the (200) surface plane where the oxygen vacancies are formed easily. From the composition analysis of Mg and O atom using synchrotron radiation photoemission spectroscopy measurement (*not shown here*), it was shown that the concentration of oxygen vacancies is higher at the low deposition rate (3Å/s).

Considering the experimental results mentioned above, it is obvious that the enhancement of SEE properties in MgO films is deeply related to the formation of oxygen vacancies at the surface of MgO film. The concentration of oxygen vacancies increased as the area of (200) plane extended because the vacancy formation energy is the lowest at the surface of (200) plane. In the Auger neutralization mechanism, maximum kinetic energy E_{max} of the emitted secondary electrons from MgO film is given by $E_{max} = E_i - 2\,\Phi_w$. Here E_i is the ionization energy of gas ion and Φ_w is the work function of the MgO film. The γ is proportional to the maximum kinetic energy E_{max} of the emitted secondary electrons. Maximum kinetic energy was obtained at the MgO surface with lowest work function. The oxygen vacancies form energy levels known as F and F^+ centers in the MgO band gap, leading to the reduction of work function of MgO. Due to decrease of MgO work function, emitted secondary electrons have maximum kinetic energy, resulting in the increase of γ.

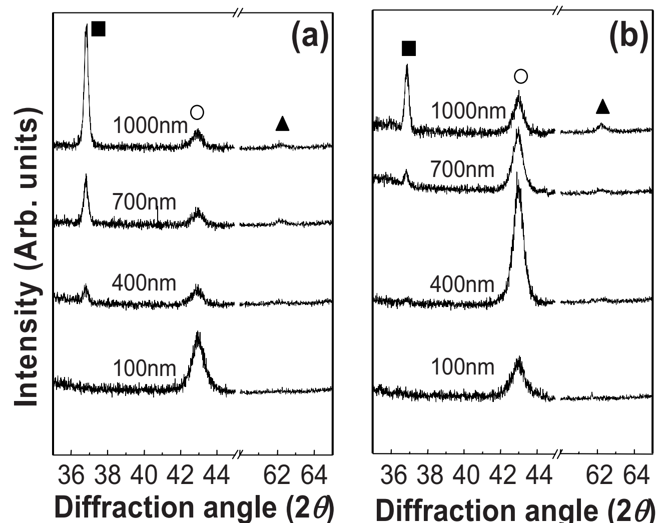

Fig. 1. Figure 1. Change of XRD profiles for the samples deposited at (a) 20Å/s and (b) 3Å/s with film thickness, (■) : MgO (111) peak, (○) : MgO (200) peak, and (▲) : MgO (220) peak.

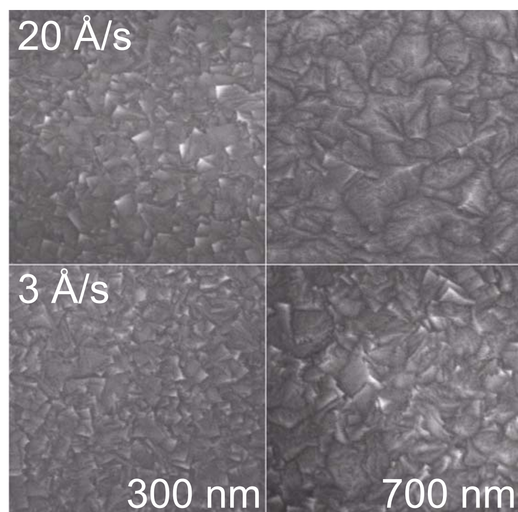

Fig. 2. FE-SEM images (× 100,000) of 300 nm, and 700 nm thickness for both deposition rates.

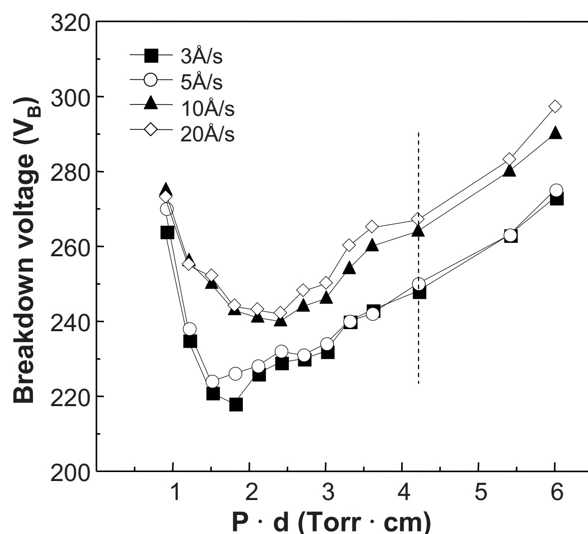

Fig. 3. Paschen curves plotted from experimental results with different deposition rates.

4. Summary

The concentration of oxygen vacancies increased as the deposition rate reduced from 20 Å/s to 3 Å/s. The oxygen vacancies deeply related to defect energy levels known as F and F^+ centers in the MgO band gap, leading to the enhancement of γ, via the reduction of work function.

Acknowledgement

This research was supported in part by the Program for the Growth Engine of Korea which was conducted by the Ministry of Commerce, Industry and Energy of the Korean Government, and in part by the Korean Research Foundation Grant funded by the Korean Government (MOEHRD) (KRF-2005-005-J13102).

5. References

1. Y. Motoyama, Y. Hirano, K. Ishii, Y. Murakami, and F. Sato, *J. Appl. Phys.* 95, 8419 (2004)

2. C. H. Ha, J. K. Kim, and K.-W. Whang, *J. Appl. Phys*. 101, 123301 (2007)

3. S. I. Ahn, S. H. Ryu, S. E. Lee, S. H. Moon, and K. C. Choi, *Jpn. J. Appl. Phys.* 46, 3579 (2007)

4. E. Y. Jung, S. G. Lee, S. H. Sohn, D. K. Lee, and H. K. Kim, *Appl. Phys. Lett*. 86, 1 (2005)